Flow Patterns in Agitated Vessels

A. B. METZNER and J. S. TAYLOR

University of Delaware, Newark, Delaware

The flow patterns obtained when viscous fluids are agitated inside baffled cylindrical tanks have been studied in both Newtonian and non-Newtonian systems. The experimental technique consisted of observing the motions of small tracer particles in highly illuminated, narrow beams of light.

The results may be broken down into two major categories. The first was a qualitative comparison between the flow patterns obtained in non-Newtonian and Newtonian fluids of the same general viscosity levels. This part of the study included observation of changes in the flow fields as one moves from laminar into turbulent conditions for both fluid systems.

The second portion of the paper deals with quantitative determinations of local flow velocities, shear rates, and power-dissipation rates in various parts of the vessel. The following conclusions may be drawn from these measurements.

1. Local fluid shear rates were found to be directly proportional to impeller speed, in both Newtonian and non-Newtonian systems. As would be expected, the shear rates decreased more rapidly with increasing distances from the impeller in pseudoplastic non-Newtonian fluids than in Newtonian systems.

2. The rates of local power dissipation decreased rapidly with distance from the impeller.

3. The fluid velocities in the horizontal plane of the impeller varied almost linearly with rotational speed in the Newtonian systems, in accordance with prior observations. On the other hand, movement in pseudoplastic systems increased exponentially with impeller speed. This effect, like the dampening of shear rates, is caused by the cumulative effects of local velocity and viscosity changes in these systems. (Increases in velocity decrease the fluid viscosity, which in turn causes further increases in velocity, etc.)

This work serves to define pertinent problems which are of importance in determining mixing rates, on a microscopic scale. Efforts may now perhaps be turned more profitably than before toward macroscopic fluid-mixing studies.

Recent investigators (5, 7) have explored the question of velocity distributions inside agitated vessels by making trace-particle photographic studies. The present study was an extension of their techniques to determine not only the velocities but also the magnitude of shear- and power-dissipation rates resulting from velocity gradients within the tank. While previous work dealt exclusively with agitation of Newtonian fluids of various viscosities, this work includes a comparison of the results from agitating both Newtonian and non-Newtonian fluids.

During agitation both mass flow around the tank and local turbulence are necessary for good mixing. First all the fluid around the tank must be moved in order that it may contact other fluids, phases, solid or gas particles, or heat transfer surfaces which may be present in the agitation vessels. Second, on a smaller scale the small local pockets of different composition, temperature, or phase must be highly sheared to ensure good blending, contact, or chemical interaction to carry out the desired process. Which part of the mixing operation is the more important from the viewpoint of over-all mixing rates depends upon the particular process in question.

While measurements of velocity distribution are most helpful in studying the rate or efficiency of the first phase of mixing, the determination of the level and distribution of shear rates may prove useful in studying some of the aspects of the second phase of the operation. A knowledge of shear rates should also prove valuable in confirming assumptions made previously in an analysis of power dissipation (2). Therefore the purposes of this work were to investigate quantitatively both factors in a common type of mixing equipment.

DESCRIPTION OF APPARATUS

The basic experimental equipment and procedure were similar to those of Sachs (5), who studied the flow patterns of water stirred with a turbine impeller. The method was essentially one of photographing illuminated trace particles in horizontal and vertical planes of light and determining the velocity distribution of the fluid for these regions from the measurement of the length of trace-particle streaks. By taking pictures of accurately known exposure times one could determine the velocity represented by the length of the streak.

A diagram of the essential parts of the apparatus is shown in Figure 1. The mixing tank was an 11.3-in. I.D. Pyrex glass cylinder cemented concentrically to the plate-glass bottom of a square, glass-enclosed outer tank. The fluid to be agitated was placed in the cylindrical tank, while water was put in between the two tanks to minimize the optical distortion caused by the curvature of the inner tank. The fluid was agitated by centrally positioned turbine impellers having six flat blades, located 4 in. from the bottom of the tank.

For most runs the tank was baffled with four 1¼-in.–wide metal strips spaced evenly at the tank wall. Flow properties were obtained with both capillary tube and rotational viscometers. Other details of the mixing and viscometric apparatus are available (2, 6).

Two different types of fluids were used in these experiments. The first was white

Karo Syrup which was determined to be a fairly viscous Newtonian fluid over the shear-rate range investigated. The other fluid was an aqueous solution of sodium carboxymethyl cellulose (CMC). The 0.7% CMC solutions had flow-behavior indexes (*1*) of 0.59 to 0.61 in the range of shear rates of interest; the flow-behavior index of the more concentrated CMC was 0.53.

The first trace particles tested were glass spheres about 0.02 in. in diameter. However since these particles have a density of about 2.3 g./cc., another lighter particle of the same size was sought and found in a Plexiglas molding powder. Most of the data were taken with the latter particles. They were nearly spherical and therefore were able to reflect light to a 90-deg. angle at all times. This last feature was considered to be absolutely necessary, for an irregularly shaped particle could be rotated in the light plane which was perpendicular to the line of sight from the camera in such a manner that the light would not be reflected from it during the full time of the exposure. It was found necessary to spray the particles with white enamel (aluminum paint is too dark) to increase their reflective properties. The Plexiglas (polymethylmethacrylate) has a density of 1.7 compared with 1.0 for the CMC solutions and 1.37 for the Karo Syrup, but because of the high viscosity of the fluids the particles continued to remain suspended for at least 5 min. in the thinnest of the solutions and for an indefinite length of time for thicker CMC solutions. It was therefore assumed that the movement of the trace particles closely represented the movement of the fluid.

Light was supplied by an arc lamp rated at 5 amp. and 115 v. However the intensity of the light was increased just before taking a photograph by increasing the no-load voltage at the source to 150 v. and drawing about 13 to 14 amp. of current briefly. Current was controlled by use of a slide-wire resistor. Originally it had been hoped that an A.C. current could have been used in the arc lamp, but the dimming of the light with the pulsation of the current was just sufficient to make the picture uncertain for analysis. Figure 1 also shows one of several slits on the sides of the tank through which the light passed and formed a nondiverging plane 3/16 in. wide.

The three views, which are pictured here, were called, respectively, *side, bottom,* and *end views* for convenience. In the side view the light enters from the side as a vertical plane which passes through the center of the tank. The impeller is then photographed at the side of the tank and perpendicular to the light plane. The side view records the image of the side of an impeller blade as shown in the sketch. The impeller for every photograph was rotating clockwise when one looked downward into the tank.

Part *b* of the same figure shows the arrangement which provided the most data. In this, the bottom view, the plane of light was horizontal. In Sachs's work it was found that the average velocity in the horizontal plane opposite the impeller blades occurred in a region just below the vertical midpoint of the impeller blade.

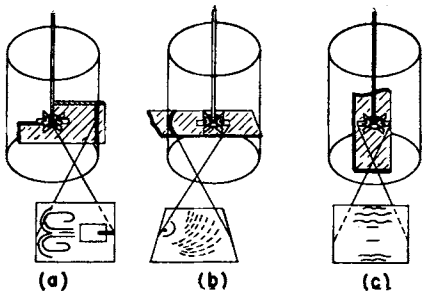

Fig. 1. Diagram of optical arrangements and mixing equipment; (*a*) side view-vertical plane, (*b*) bottom view-horizontal plane, (*c*) end view-vertical plane.

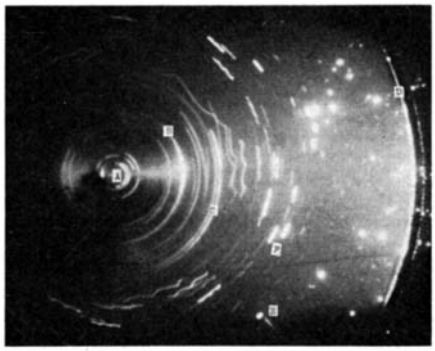

Fig. 2. Bottom-view photograph; fluid: 1.2% CMC solution, Reynolds number: 7.7, rotational speed: 60 rev./min., impeller size: 4 in. Legend: (*A*) center of impeller, (*B*) edge of stabilizing disk, (*C*) trace from tip of impeller blade, (*D*) edge of tank, (*E*) reflection from baffle, (*F*) trace-particle streak.

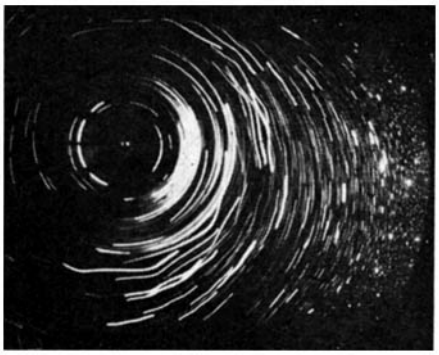

Fig. 3. Bottom-view photograph; fluid: Karo Syrup, Reynolds number: 6.2, rotational speed: 60 rev./min., impeller size: 4 in.

Therefore, to simplify the problem a thin plane in this region was the one illuminated for most of the data taken from the bottom view. In order to facilitate the focusing, a first-surface mirror was mounted just below the mixing tank, and all data were taken from photographs of the reflected image.

Part *c* of Figure 1 illustrates the end view. For this view a vertical plane of light about ⅜ in. thick was used. The light was reflected off a mirror, since convection currents from the burning arc carried both heat and ashes to the bottom of the glass tank when the lamp was placed directly beneath it. In this case the photograph was taken through the front side of the tank to record the image of the tip end of the impeller at a time when it was pointing toward the camera and in the vertical plane of light. The tip of the blade was thereby illuminated inwardly for a distance of about ⅜ in. so that trace particles in this region might be photographed. A small amount of quantitative as well as qualitative data were taken from this view.

A view camera with an f/4.7 lens was used to take the still pictures. Photographs of from one to ten exposures were taken with the position of the impeller in relation to the camera fixed for each exposure by the use of a solenoid-operated shutter. The shutter was tripped at the proper time by a cam mounted on the impeller shaft closing a microswitch and thereby activating the solenoid. The position of the image of the impeller could be set by fixing the position of the cam. Twelve volts supplied by dry cells were used, since the normal 6 v. were not quite enough to assure sufficiently rapid action of the solenoid. A toggle switch was also inserted into the circuit so that the shutter, once it had been cocked, would be closed only when desired.

Exposure times varied between 1/60 and ½ sec. All negatives were processed in a D-19 high-contrast developer for 15 min. Although additional intensification of the negative was considered several times for the CMC photographs, it was decided to be an unwise procedure since the probable result would have been an even greater increase in the background haze, which was already quite high. Were it merely a question of improper lighting, intensification might have helped, but the haziness around the image could not be overcome by this procedure.

DISCUSSION OF QUALITATIVE DATA

Figure 2 is a representative example of the bottom view in non-Newtonian fluid systems. It is apparent for this case ($N_{Re} = 7.7$, laminar region) that most of the flow is restricted to the neighborhood of the turbine blades. Perhaps the most interesting part of the photograph is the scalloped shape of the trace-particle streaks. This effect is undoubtably caused by flow over, around, and then behind the blade as it passes through the fluid. The three ridges on the trace-particle streaks are of course caused by the passage of three of the turbine blades during the ½-sec. exposure time. The disturbance is also propogated radially through the plane of liquid. However, there is no radial component of flow, the pattern having merely a net circular motion.

Figure 3 shows the flow pattern for Karo Syrup at the same rotational speed and nearly the same Reynolds number as Figure 2. It is obvious that the amount of fluid movement is greater, that the fluid velocities are larger, and that the motion in this case

extends almost to the periphery of the tank. The reasons for these differences will be discussed later is some detail.

A comparison of Figure 2 with Figure 4 shows how the radial component of velocity develops as the rotational speed of the impeller is increased. The fluid movement is now sufficient to extend to, and be influenced by, the baffles. Even at this higher impeller speed the absence of streaks near the wall shows that there is still little or no fluid movement here. The Reynolds number of 28 is just at the lower end of the transition range for these more concentrated CMC solutions (2).

Figures 5 and 6 show the early development of the usual mixing flow pattern in Karo Syrup, occurring just at the end of the laminar region. In Figure 6 the effect on the flow pattern of the baffle, which is clearly visible on the right of the photograph, is evident. In Figure 5 one sees the vortices being formed (above and below the plane of the turbine) which cause the transport of fluid and the beginning of real fluid turnover throughout the entire tank. The bottom view shows how the scalloped or saw-tooth effect from the flow over the blade has been propogated to the very edge of the tank. By contrast, Figure 4 for CMC (with nearly three times as high a Reynolds number) showed that flow was still entirely confined to the center of the tank for this pseudoplastic non-Newtonian fluid.

It is now apparent that the radial flow increases with increasing rotational speed and that as a corollary the total rate of fluid turnover within the tank increases. Likewise it was observed that the non-Newtonian CMC shows much less flow and lower velocities than does Karo Syrup under the conditions of the same rotational speed and similar Reynolds number, although small-scale mixing due to high shear rates may be greater near the impeller.

One has also observed the effect on the flow pattern upon going from the laminar into the early transition range as defined by the power number–Reynolds number correlation (2, 4). One effect of this change has been the creation of a radial component of velocity. However, Figures 7 and 8 show that a radial component of velocity can exist in both CMC and Karo Syrup even when Reynolds numbers are in the laminar region. Figure 7 shows a 2-in. turbine rotating at 200 rev./min. in 1.2% CMC. Although the actual flow is small, a definite radial component is present at the Reynolds number of 11. Figure 8 compares similar conditions in Karo Syrup, where the flow is much larger. In this picture no baffles are present, but, since the flow only extends to the position of their inner limit, this fact is not important.

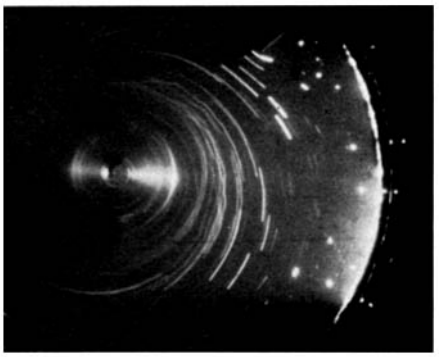

Fig. 4. Bottom-view photograph; fluid: 1.2% CMC solution, Reynolds number: 28, rotational speed: 150 rev./min., impeller size: 4 in.

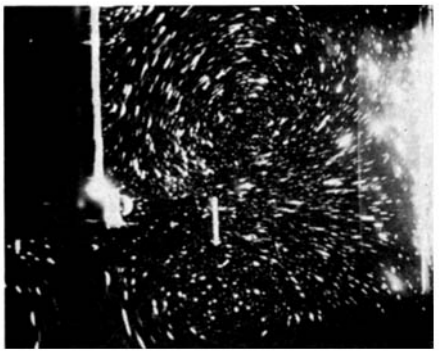

Fig. 5. Side-view photograph; fluid: Karo Syrup, Reynolds number: 10.3, rotational speed: 100 rev./min., impeller size: 4 in.

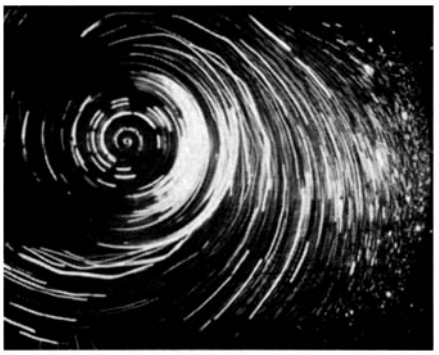

Fig. 6. Bottom-view photograph; fluid: Karo Syrup, Reynolds number: 10.3, rotational speed: 100 rev./min., impeller size: 4 in.

Although the Reynolds number has appeared to be useful in correlating the power for all fluids and impeller sizes (2, 4), it is apparent that the flow patterns for Newtonian and non-Newtonian fluids may be very different. While Figures 2 and 3 have similar laminar-region Reynolds numbers, both the velocity and the extent of the flow are much greater in Karo Syrup. Other figures (6) show that this situation continues into the transition region. Not only may a difference in the type of fluid produce a change in the flow pattern for the same Reynolds number, but Figure 7 compared with Figures 2 and 4 (which bracket it in regard to Reynolds number) shows that a change in the size of impeller may have a similar effect in non-Newtonian systems. Since each impeller was dimensionally similar, it is seen that even though one maintains the Reynolds number constant during scale up, this provision alone does not necessarily signify similar flow patterns in the model and prototype.

Figures 9 and 10 show, respectively, the bottom and end views of a 1.2% CMC solution for a rotational speed of 150 rev./min*. At the Reynolds number of 78 the flow is well into the transition region and the radial velocity component is high. The end view shows how the flow at the top (and bottom) of the blade now includes an inflowing vertical component. Figures 11 and 12 compare side-view conditions for 1.2% CMC and Karo Syrup at the highest impeller speeds recorded. Generally the two fluids are exhibiting the same general flow pattern, but there are several important differences.

While stirring low-viscosity fluids such as water, Sachs and Rushton (5) found that the vertical inflow of fluid (as shown in Figure 5) into the disklike jet issuing from the impeller contributes about 50% of the total flow of this stream. In the case of the pseudoplastic CMC solution in the above-mentioned photographs the fluid has effectively thinned out in this jet region owing to the high shear rates. Quantitative data indicate that for Figure 11 there may actually be more flow with the 1.2% CMC than with the Karo Syrup. In order for the vertical stream to feed the jet sufficiently, the vortexes above and below this stream form some distance away from the impeller.

The last series of photographs shows the beginning of well-developed turbulence, as evidenced by the fact that the path lines appear to be twisting and to cross frequently. Some of the following data indicate that the turbulence, in some cases at least, may originate above or below the moving blades rather than between them. The fluid which is being displaced by the blades in the vertical direction must be moving counter to the inflow from above and below in the region immediately ahead of the rotating blade. The flow up and over the blade then quickly changes direction as the blade passes by, flowing in behind it in a direction now parallel or coincident with the vertically inflowing stream. Figures 13 for Karo Syrup and 14 for 0.7% CMC show that this momentary outward oscillation of fluid has created a disturbance in the incoming fluid above and below the plane of the impeller. In

* Figures 9 to 13, 20, and 22 to 25 have been deposited with the American Documentation Institute, Photoduplication Service, Library of Congress, Washington 25, D. C. Copies are available as document 6051 for $2.50 for photostats and $1.75 for microfilm.

Fig. 7. Bottom-view photograph; fluid: 1.2% CMC solution, Reynolds number: 11, rotational speed: 200 rev./min., impeller size: 2 in.

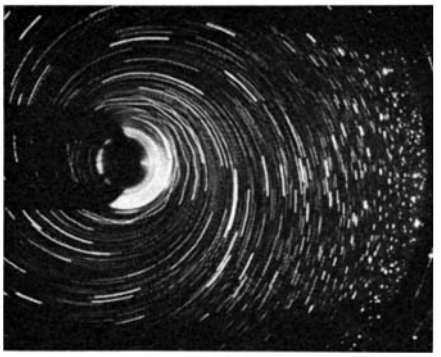

Fig. 8. Bottom-view photograph; fluid: Karo Syrup, Reynolds number: 5.15, rotational speed: 200 rev./min., impeller size: 2 in.

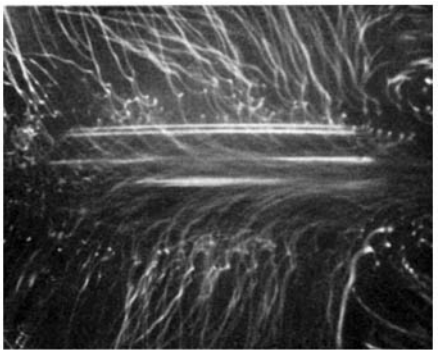

Fig. 14. End-view photograph; fluid: 0.7% CMC solution, Reynolds number: 450, rotational speed: 300 rev./min., impeller size: 6 in.

addition the high radial velocities cause the direction of the flow of the turbine discharge stream to become parallel to the impeller blades. In this case one must expect a considerable disturbance at the tip of the blade caused by the large difference in velocities between the end of tthe blade and the tangential velocity components of the neighboring stream of fluid.

Figure 15 is the bottom view which matches Figure 14. The exposure time in this case has been reduced to 1/5 sec. to minimize the haziness from the turbidity of the fluid and thereby more clearly show the turbulence which extends nearly to the wall.

It is probable that turbulence may begin in the pseudoplastic material before it does in Newtonian fluids, since shear rates are higher near the impeller (this is proven by later quantitative measurements). These higher shear rates result from the decrease in apparent viscosity of the non-Newtonian fluid and in turn lead to even greater reductions in fluid viscosity. Therefore, viscous dampening influences are greatly reduced near the impeller in pseudoplastic fluid systems. However, since the shear rate rapidly drops off and the apparent viscosity simultaneously increases as the flow progresses radially out from the impeller, this observed turbulence may be quickly dampened out. Figure 16 shows the dilute (0.7%) CMC solution being agitated at 400 rev./min. by the smaller 4-in. impeller. In this case the turbulent condition of the flow observed near the impeller changes to laminar and smooths out rapidly as the fluid proceeds further out into the tank.

It is possible, therefore, to have both laminar and turbulent regions in the mixing tank at the same time. This condition can probably occur in both Newtonian and non-Newtonian fluids, at least in the upper transition region. This fact, therefore, makes analysis of power input, flow, and mixing efficiency very difficult and would appear to indicate a considerable limitation to correlations based on over-all average conditions such as the Reynolds number.

QUANTITATIVE RESULTS

The particle streaks on photographs similar to Figures 2 to 16 were measured to obtain quantitative data on fluid velocities as a function of position within the tank. These velocities were differentiated to obtain the local shear rates, and finally the local rates of power dissipation were obtained by multiplying the observed shear rates by the corresponding shear stress, as obtained from the viscometric data. Fluctuating point velocities may not be given accurately under highly turbulent conditions by the photographic technique used, but in this work any turbulence present was sluggish and accurate results were readily obtainable.

Figures 17 to 19 show the shear-rate distribution in the horizontal plane just below the center of the impeller. It may be seen from these curves that the shear rate was highest near the impeller but that it fell off rather rapidly as one proceeded radially out into the body of the fluid. For both the Newtonian and the non-Newtonian fluid the shear rate appeared to be directly proportional to the rotational speed at all distances between the tip of the impeller and the wall of the tank. This is one of the major results sought in the present study, as it constitutes the first direct confirmation of the relationship used to correlate power consumption in non-Newtonian systems (2).

Comparison of the available data for two different impeller sizes with the same fluid show in the case of CMC that the shear rate at a given distance from the impeller is slightly greater for the larger impeller. Although the data for Karo Syrup were not as consistent, a comparison showed that the difference in shear rate is even larger in this case (6). These results indicate that the earlier (2) assumption that the average shear rates depend only on impeller speed may possibly break down under conditions of very large changes in impeller diameter. Since this effect of impeller diameter seems to be more important for Karo Syrup than CMC, other types of non-Newtonian fluids (that is dilatant fluids) may give even greater changes if this trend of increased differences with increases in the flow-behavior index continues. Should this actually turn out to be the case the earlier assumption (2) that the shear rate is a function only of impeller speed would have to be modified to include effects of diameter and flow-behavior index. However, the fact that the diameter effects appear to decrease with increasing pseudoplasticity (flow-behavior indexes approaching zero) indicates that extrapolations of the power correlation should be readily possible to larger diameters in highly pseudoplastic and Bingham plastic fluids.

Shear-rate data taken in a vertical plane, by use of end-view photographs, were similar to the results shown in Figures 17 to 19.

The second factor of interest (local rates of power dissipation) is shown in Figures 20 to 22 as a function of the actual radial distance from the tip of the impeller blade. On the same figures the horizontal dashed lines at each rotational speed give the value of the *average* rate of power dissipation. These were determined by dividing the volume of agitated fluid into the power input to the entire tank as measured with a dynamometer. At speeds up to about 150 rev./min. it is seen that the position at which the *point*, or *local*, power-dissipation rate drops to the level of the average power-consumption rate moves radially outward, especially in the case of the CMC. This is a result of the very incomplete mixing at the lowest speeds, as noted in Figures 2 and 3. Therefore, within this range, as the speed is increased the region in which the power-dissipation

rate is appreciable rapidly spreads outward from the immediate vicinity of the impeller. In other words, the mixing rates become more nearly equal in all parts of the tank as the completely unmixed region decreases in volume.

Above about 150 rev./min. (Reynolds numbers of the order of 10 to 100) one moves well into the transition region as defined by the power number-Reynolds number plots. Figures 20 to 22 show that in this region progressive increases in impeller speed tend to make the mixing process less uniform again; a large fraction of the incremental increase in power input is dissipated in the immediate vicinity of the impeller. As a result the intersection of the dashed and solid lines moves progressively closer to the impeller. In this region one has excellent fluid turnover throughout the entire tank (Figures 11, 12, 15, 16), but the level of shear rates or local power-dissipation rates is still not high except in the immediate vicinity of the impeller. In fact, the level of turbulence is so markedly low everywhere except in the region of the impeller that in more recent work (3) a model which assumes very low turbulence everywhere except in the immediate vicinity of the impeller has served to correlate mixing rates over a remarkably wide range of conditions.

This condition of nonuniformity is greater in the CMC solutions. The decrease in apparent viscosity around the impeller causes a much higher degree of shearing or turbulence in that region. Conversely, the rapid decrease in shear rates as one moves away from the impeller increases the viscosity of the fluid, which in turn dampens the velocities and their fluctuations even more. As a result, pseudoplastic non-Newtonian fluids represent an extreme case of a nearly perfect mixing zone near the impeller combined with very little mixing in other parts of the system.

Figures 23 to 25 show the velocity distributions within the vessel at the plane of the impeller. Comparison of Figures 23 and 24 shows a considerable difference between the velocity changes with increasing rotational speed for the two fluids. In the Newtonian fluid the velocity for every distance parameter appeared to vary almost linearly with rotational speed, except for the tendency toward curvature at 400 rev./min. On the other hand, the data for the pseudoplastic CMC solution showed a very large amount of curvature with increasing speed for both the 4- and 6-in. impellers. It is also apparent that at every distance shown, flow velocities were higher for the agitated Karo Syrup solutions than for 1.2% CMC solutions. Although the agitated 1.2% CMC solutions have a lower apparent viscosity near the impeller where the shear rates are high, the data and qualitative observations indicate that the great bulk of the fluid in the tank away from the impeller has shear rates less than the 4 to 6 sec.$^{-1}$ where the flow curves of the two fluids cross. As a result of this fact the pseudoplastic is effectively more viscous except near the impeller, and less circulation of fluid occurs at a given rotational speed. In the laminar region the differences in shear rate and fluid motion for CMC are very large. Therefore, the fluid near the impeller rotates much like a solid cylinder rotating in a bearing, with a lubricating layer of highly sheared, but otherwise nearly stagnant, fluid just out from the tip of the impeller. As the speed of the impeller was increased, the centrifugal forces acting on the fluid cause radial flow, and, as more of the fluid gains motion, the resulting local shear rates in CMC decrease the apparent viscosity in these regions of fluid movement. As a result of the decrease in viscosity with increasing shear rate, the amount of fluid motion (and the velocity of this motion) increases at a rate which is greater than directly proportional to the rotational speed. The convergence of the velocity data for the two fluids indicates that for higher rotational speeds (about 500 to 600 rev./min.) at least some of the local velocities for the 1.2% CMC solution will exceed those of Karo Syrup. Owing to the greater amount of fluid movement using the 6-in impeller (Figure 25) there is an even greater rate of curvature in this case.

A brief investigation was also made of the variations in velocity with respect to the angular position of the blades of the impeller (6). Except at radii close to the radius of the tips of the blades, these differences were not found to be large, however, and no further detailed study was undertaken.

CONCLUSIONS

1. In both Newtonian and non-Newtonian systems the fluid shear rates were found to be directly proportional to the rotational speed of the impeller under all conditions studied. This fact is of primary importance in supporting the basis for correlation of agitation power requirements in non-Newtonian systems.

The only indication of conditions under which the above direct proportionality might be affected by other variables was obtained by varying the impeller diameter. As a result, it appears at least possible that the earlier correlation of power requirements (2) should not be extrapolated to impellers which are greatly larger than those studied, except for very highly pseudoplastic fluids.

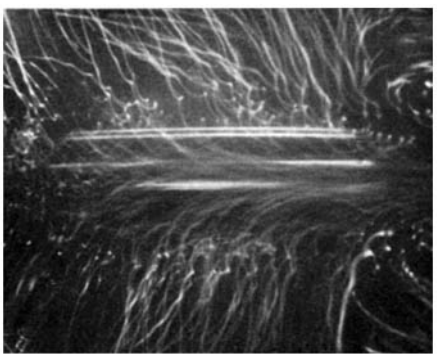

Fig. 15. Bottom-view photograph; fluid: 0.7% CMC solution, Reynolds number: 450, rotational speed: 300 rev./min., impeller size: 6 in.

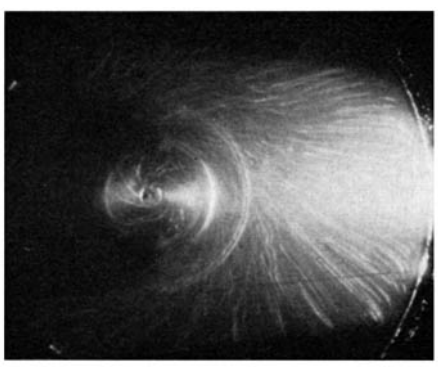

Fig. 16. Bottom-view photograph; fluid: 0.7% CMC solution, Reynolds number: 310, rotational speed: 400 rev./min., impeller size: 4 in.

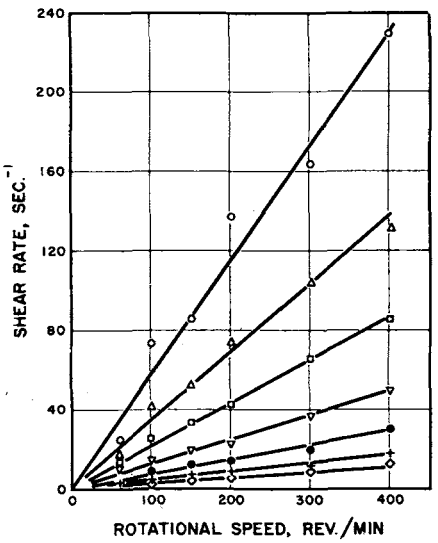

Fig. 17. Shear-rate distriubtion in Karo Syrup, horizontal plane, 4-in. impeller.

Symbol	Distance (radially) from tip of impeller
⊙	Impeller tip
△	0.10 in.
⊡	0.20 in.
▽	0.34 in.
⊗	0.50 in.
+	1.00 in.
◇	1.70 in.

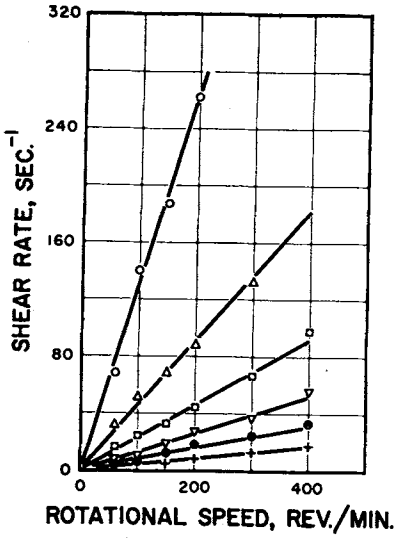

Fig. 18. Shear-rate distribution in 1.2% CMC solution, 4-in. impeller. Other conditions and symbols as in Figure 17.

2. High rates of shearing and power dissipation occur close to the impeller. Within the laminar region the large differences between the rates of power dissipation close to the impeller and elsewhere in the tank decrease with increasing impeller speed, since such speed increases serve to bring some slight mixing to other parts of the tank. At higher speeds (within the transition region) the reverse, however, appears to be true: any incremental increases in power input are to a large extent consumed in the immediate region of the impeller. Under conditions of good mixing a simplified model of the overall process would appear to be that in which one assumes essentially all the highly turbulent mixing to be confined to the region of the impeller, with fluid motion elsewhere in the tank serving primarily to bring fresh fluid into this region.

3. Under laminar-flow conditions relatively little agitation takes place within the mixing tank. The flow is generally circular in motion and confined to the region near the impeller.

4. In the first half of the transition range the radial velocity component increases with rotational speed (and Reynolds number) quite rapidly. In this region over-all circulation of fluid and subsequent mixing begin within the tank. The mixing is carried out by the transport and blending of fluid and not as yet by any noticeable turbulence.

5. As the rotational speed approaches the middle of the transition region ($N_{Re} \approx 100$) some turbulence becomes visible on the photographs. This condition begins near or between the blades of the impeller.

Local turbulence, particularly in pseudoplastics, is rapidly dampened out in a short distance. The decrease in viscosity near the impeller where the shear rates are highest advances the formation of turbulence in this region in pseudoplastic fluids.

6. In the horizontal plane of the impeller, velocities increase only slightly more rapidly than linearly with rotational speed in the Newtonian fluids. However in the pseudoplastic fluid the velocities increase more nearly exponentially with increases in impeller speed as a result of the reduction of the apparent viscosity of the fluid with increasing shear rate. Under conditions of high shear rate and turbulence, pseudoplastics may undergo greater over-all flow with less total power imput than for Newtonian fluids having similar apparent viscosities at lower shear rates. At lower rotational speed and lower shear rates the opposite conditions may exist.

These conclusions are all based on a study under a limited range of conditions. One tank, 11.3 in. in diameter, was employed. Dimensionally similar flat-blade turbines ranging from 2 to 6 in. in diameter were used. Rotational speeds of from 60 to 600 rev./min. were studied providing a Reynolds-number variation of from 2.1 to 450, which covered the laminar region and most of the transition region. The conclusions are, therefore, most valid for this range of conditions.

ACKNOWLEDGMENT

This work was supported by the Office of Ordnance Research, U. S. Army.

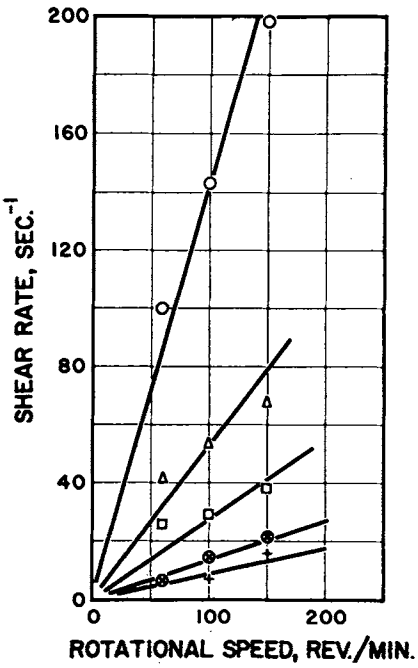

Fig. 19. Shear-rate distribution in CMC, 6-in. impeller. Other conditions and symbols as in Figure 17.

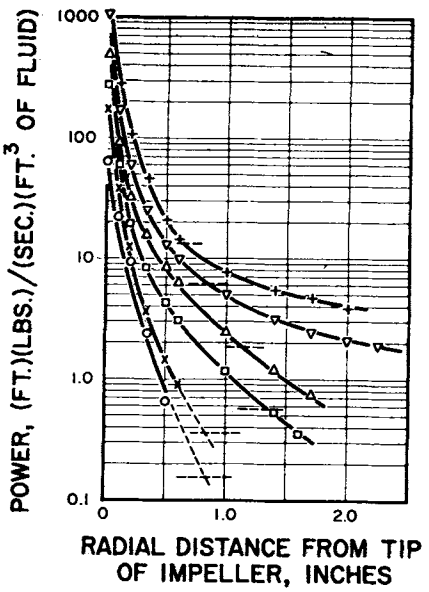

Fig. 21. Local or point power-dissipation rates. 1.2% CMC, 4-in. impeller.

Legend:
- ⊙ 60 rev./min.
- × 100 rev./min.
- □ 150 rev./min.
- △ 200 rev./min.
- ▽ 300 rev./min.
- \+ 400 rev./min.

NOTATION

- du/dr = fluid shear rate, sec.$^{-1}$
- D = impeller diameter, ft.
- N = rotational speed of impeller, rev./sec.
- N_{Re} = Reynolds number, dimensionless, defined as $D^2N\rho/\mu$ for Newtonian fluids and $D^2N\rho/\mu_a$ for others; apparent viscosity μ_a is evaluated at a shear rate du/dr equal to $13N$ (2)
- μ = viscosity, lb.-mass/sec.ft.
- ρ = fluid density, lb.-mass/cu.ft.

LITERATURE CITED

1. Metzner, A. B., and J. C. Reed, *A.I.Ch.E. Journal*, 1, 434 (1955); A. B. Metzner, in "Advances in Chemical Engineering," Vol. 1, Academic Press, New York (1956).
2. ———, and R. E. Otto, *A.I.Ch.E. Journal*, 3, 3 (1957).
3. Norwood, K. W., Ph.D. thesis. Univ. Delaware, Newark (1959).
4 Rushton J. H., and J. Y. Oldshue, *Chem. Eng. Progr.*, 49, 161 and 267 (1953).
5. Sachs, J. P., and J. H. Rushton, *ibid.*, 50, 597 (1954).
6. Taylor, J. S., M.Ch.E. thesis, Univ. Delaware, Newark (1955).
7. Tennant, B. W., Thesis, Illinois Inst. Technol., Chicago (1952).

Manuscript received November 7, 1958; revision received April 30, 1959; paper accepted May 6, 1959. Paper presented at A.I.Ch.E. Cincinnati meeting.